Progress In Electromagnetics Research, Vol. 143, 263–284, 2013

A DRESSED-STATE ASSISTED LEFT-HANDED COHERENT MEDIUM FOR HIGH-GAIN OPTICAL AMPLIFICATION

Jian Qi Shen[1, 2, *]

[1]Centre for Optical and Electromagnetic Research, State Key Laboratory of Modern Optical Instrumentations, East Building No. 5, Zijingang Campus, Zhejiang University, Hangzhou 310058, China

[2]Joint Research Centre of Photonics of the Royal Institute of Technology (Sweden) and Zhejiang University, Zijingang Campus, Zhejiang University, Hangzhou 310058, China

Abstract—A scheme of double-negative left-handed atomic vapor medium based on dressed-state assisted simultaneous electric and magnetic resonances is suggested. In this mechanism, simultaneous electric- and magnetic-dipole allowed transitions of atoms are driven by an optical wave by taking full advantage of both mixed-parity *dressed-state assisted resonance* and *incoherent population pumping* in a quantum-coherent atomic medium (e.g., alkali-metal atomic vapor). Since the simultaneously negative permittivity and permeability can be achieved in a same frequency band, such an atomic vapor will exhibit an incoherent-gain double-negative refractive index that is three-dimensionally isotropic and homogeneous. The imaginary part of the negative refractive index of the present atomic vapor would be drastically suppressed or would become negative because of loss compensation through incoherent population transfer. The quantum-coherent left-handed atomic vapor presented here will have four characteristics: *i*) three-dimensionally isotropic and homogeneous negative refractive index, *ii*) double-negative atomic medium at visible (and infrared) wavelengths, *iii*) tunable negative refractive index based on dressed-state quantum coherence, and *iv*) high gain due to incoherent pumping action.

Received 8 June 2013, Accepted 10 October 2013, Scheduled 4 November 2013

* Corresponding author: Jian Qi Shen (jqshen@zju.edu.cn).

1. INTRODUCTION

The artificial metamaterials (including negatively refracting media) have offered a new kind of materials for exploration of many fundamental and interesting electromagnetic and optical effects [1–4], including some attractive properties that dramatically modify conventional optical phenomena of electromagnetic media [5–10]. Though there must have been some new techniques for realizing isotropic metamaterials [11–13], yet fabrication of ideally three-dimensionally isotropic and homogeneous negatively refracting materials is believed to be still a challenging issue [14–16]. Obviously, the impact would be enormous if an isotropic and homogeneous material of simultaneously negative permittivity and permeability can be realized by using new scenarios such as quantum optical approach [17–20], in which photonic resonance and quantum coherence are involved [21–23]. In the approaches of quantum coherence, however, there are two bottlenecks that should be resolved in order to realize simultaneously negative permittivity and permeability: *i*) It would be difficult in finding suitable atomic level structures that can give rise to *simultaneous* electric- and magnetic- dipole allowed transitions. That is to say, it would not be so easy to obtain the *simultaneous* on-resonance transitions for achieving *simultaneously* negative permittivity and permeability, since, in almost all the atoms, any electric- and magnetic-dipole transition frequencies in any atomic systems of various configurations are in principle not equal; *ii*) Loss in the quantum-coherent left-handed media [17–20] is often quite large (e.g., the magnitude of the imaginary part of the refractive index is close to the magnitude of its real part, i.e., Im $n \simeq |\text{Re } n|$), and such negatively refracting materials would in fact be not realistic for practical applications. Here, we shall overcome these two bottlenecks by using a dressed-state assisted quantum-coherent double-negative gaseous atomic medium. We will suggest a different scheme of quantum coherence [17–20] for realizing the negative refractive index, which takes full advantage of pumped mixed-parity transitions for achieving the simultaneous electric- and magnetic-dipole responses. This will lead to a three-dimensionally isotropic gain medium of negative refractive index.

A dressed atomic level has mixed parity since it is a linear superposition of two pure-parity levels (bare levels of atoms), and this will give rise to the simultaneous electric- and magnetic-dipole allowed transitions between the *dressed levels* and some other pure-parity *bare levels*. Then both the electric and the magnetic fields of an applied probe beam can be resonant with this dressed-state assisted

transition. Besides, an optical pumping (an incoherent pumping action for population transfer) [24–26] will be utilized for overcoming losses in this negatively refracting atomic vapor. Thus, a new scenario of negative refractive index at visible wavelengths can be proposed based on the present scheme, where the imaginary part of the negative refractive index would be drastically suppressed and high-gain optical amplification will result due to the incoherent pumping action.

2. MIXED-PARITY TRANSITION OF DRESSED STATES

Consider a four-level atomic system $\{|1\rangle, |2\rangle, |a\rangle, |b\rangle\}$ in Fig. 1. We assume the two upper bare levels $|a\rangle, |b\rangle$ have opposite parities and the ground level $|1\rangle$ has an even parity. For example, level $|a\rangle, |b\rangle$ and $|2\rangle$ possess even, odd and odd parities, respectively. Such an atomic system $\{|1\rangle, |2\rangle, |b\rangle, |a\rangle\}$ can be found in neutral alkali-metal atoms, e.g., the neutral rubidium

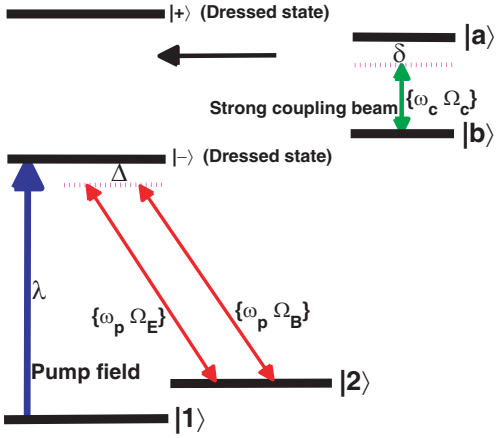

Figure 1. The schematic diagram for the pumped dressed-state mixed-parity transitions. The electric-dipole allowed transition $|a\rangle$-$|b\rangle$ is driven by a strong coupling laser beam, and two dressed states $|+\rangle$ and $|-\rangle$ will result from the linear combinations of the two bare levels $|a\rangle$ and $|b\rangle$. The energy level pair $|2\rangle$-$|-\rangle$ is coupled to the electric and magnetic fields of a probe beam whose electric and magnetic Rabi frequencies are Ω_{E} and Ω_{B}, respectively. Both electric- and magnetic-dipole allowed transitions (between the bare level $|2\rangle$ and the mixed-parity dressed level $|-\rangle$) will occur, and hence simultaneously negative permittivity and permeability would be achieved through the pumped dressed-state transitions.

atomic system $\{5^2S_{\frac{1}{2}}, 5^2P_{\frac{1}{2}}, 5^2P_{\frac{3}{2}}, 4^2D_{\frac{3}{2}}\}$ with the energy levels $\{0.000, 12578.950, 12816.545, 19355.649\}\,\mathrm{cm}^{-1}$ [27] can serve as such a system. Here, the transition frequency between level $5^2P_{\frac{1}{2}}$ and level $5^2P_{\frac{3}{2}}$ is $2\pi c\times(12816.545-12578.950)\,\mathrm{cm}^{-1}$, i.e., $4.5\times10^{13}\,\mathrm{s}^{-1}$. Besides, the neutral cesium atomic system $\{6^2S_{\frac{1}{2}}, 6^2P_{\frac{1}{2}}, 6^2P_{\frac{3}{2}}, 7^2S_{\frac{1}{2}}\}$ with the energy levels $\{0.000, 11178.2686, 11732.3079, 18535.529\}\,\mathrm{cm}^{-1}$ [28], where the transition frequency between level $6^2P_{\frac{1}{2}}$ and level $6^2P_{\frac{3}{2}}$ is $1.0\times10^{14}\,\mathrm{s}^{-1}$, can also be applicable to our scenario of dressed-state assisted negative refractive index. Some other metallic atomic systems, e.g., the neutral mercury atomic system $\{6^1S_0, 6^3P_0, 6^1P_1, 7^3S_1\}$ with the energy levels $\{0.000, 37645.080, 54068.781, 62350.456\}\,\mathrm{cm}^{-1}$ [29], in which the transition frequency between level 6^3P_0 and level 6^1P_1 is $3.1\times10^{15}\,\mathrm{s}^{-1}$, can also be employed in the present mechanism of atomic-vapor negative refraction. In a word, the dressed-state assisted double-negative coherent atomic vapors can exhibit their three-dimensionally isotropic negative refractive index at visible and infrared wavelengths. This is one of the attractive features of the present scheme.

We shall now explain the mixed-parity transition of the dressed states. The electric-dipole allowed transition $|a\rangle$-$|b\rangle$ is driven by a strong coupling laser beam, and this will lead to two orthogonal dressed states $|+\rangle$ and $|-\rangle$. These orthogonal dressed states are the linear combinations of the two bare levels $|a\rangle$ and $|b\rangle$, i.e.,

$$\begin{cases} |+\rangle = \cos\vartheta|a\rangle + e^{\mathrm{i}\phi}\sin\vartheta|b\rangle, \\ |-\rangle = -\sin\vartheta|a\rangle + e^{\mathrm{i}\phi}\cos\vartheta|b\rangle, \end{cases} \tag{1}$$

where the coefficients $\sin\vartheta$ and $\cos\vartheta$ are so defined that $\sin^2\vartheta = (1-1/\sqrt{4\Omega_{\mathrm{c}}^2/\delta^2+1})/2$, $\cos^2\vartheta = (1+1/\sqrt{4\Omega_{\mathrm{c}}^2/\delta^2+1})/2$, respectively. Here, the dressed-state phase parameter $\phi = \arg[-p_{ab}\mathcal{E}_{\mathrm{c}}]$ and the Rabi frequency, Ω_{c}, of the coupling field is $p_{ab}\mathcal{E}_{\mathrm{c}}/\hbar$, where $\mathcal{E}_{\mathrm{c}}$ denotes the slowly-varying amplitude (envelope) of the strong coupling field. For a more general and detailed review on the atomic dressed states, readers can be referred to Haroche's references [30, 31]. In what follows, we shall use the dressed states to achieve the mixed-parity electromagnetic transitions. For simplicity, we suppose that the phase parameter $\phi = 0$. Obviously, the frequencies, ω_a and ω_b, which correspond to the energy levels of $|a\rangle$ and $|b\rangle$, are $\omega_a = \bar{\omega} + (\omega_{\mathrm{c}}+\delta)/2$ and $\omega_b = \bar{\omega} - (\omega_{\mathrm{c}}+\delta)/2$, respectively. Here, $\bar{\omega} = \omega_2 + \omega_{b2} + (\omega_{\mathrm{c}}+\delta)/2$ with ω_{b2} the transition frequency between level $|2\rangle$ and level $|b\rangle$ (i.e., $\omega_{b2} = \omega_b - \omega_2$) and ω_{c} the mode frequency of the coupling field. The dressed-state $|-\rangle$-$|+\rangle$ transition frequency is $\omega_{+-} = \omega_{\mathrm{c}} + \sqrt{\delta^2+\Omega_{\mathrm{c}}^2}$, which involves a

modification compared with the bare-level $|b\rangle$-$|a\rangle$ transition frequency ω_{ab} ($\omega_{ab} = \omega_{\rm c} + \delta$). Apparently, the frequencies, ω_+ and ω_-, which correspond to the energy levels of $|+\rangle$ and $|-\rangle$, are of the form

$$\begin{aligned} \omega_+ &= \bar{\omega} + \frac{1}{2}\left(\omega_{\rm c} + \sqrt{\delta^2 + \Omega_{\rm c}^2}\right), \\ \omega_- &= \bar{\omega} - \frac{1}{2}\left(\omega_{\rm c} + \sqrt{\delta^2 + \Omega_{\rm c}^2}\right), \end{aligned} \tag{2}$$

respectively. Define the electric and magnetic dipole moment matrix elements: $\mathbf{p}_{-,2} = \int_V \phi_-^* e\mathbf{r}\phi_2 {\rm d}V$, $\mathbf{m}_{-,2} = \int_V \phi_-^* \frac{e}{2m}(\mathbf{L} + 2\mathbf{S})\,\phi_2 {\rm d}V$, where ${\rm d}V$ denotes the volume element. Further calculation shows that the relations between the dressed-state electric and magnetic dipole moment elements $\mathbf{p}_{-,2}$, $\mathbf{m}_{-,2}$ and the pure-parity counterparts $\mathbf{p}_{a2}$, $\mathbf{m}_{b2}$ are given by

$$\begin{aligned} \mathbf{p}_{-,2} &= \langle -|e\mathbf{r}|2\rangle = -\mathbf{p}_{a2}\sin\vartheta, \\ \mathbf{m}_{-,2} &= \left\langle -\left|\frac{e}{2m}(\mathbf{L} + 2\mathbf{S})\right|2\right\rangle = \mathbf{m}_{b2}\cos\vartheta, \end{aligned} \tag{3}$$

respectively.

Now the four-level bare-state system $\{|1\rangle, |2\rangle, |a\rangle, |b\rangle\}$ becomes a new four-level system $\{|1\rangle, |2\rangle, |+\rangle, |-\rangle\}$, where the dressed states $|\pm\rangle$ have mixed parities. Thanks to the mixed parity of the dressed state $|-\rangle$, now the electric-dipole moment $\mathbf{p}_{-,2}$ and the magnetic-dipole moment $\mathbf{m}_{-,2}$ no longer vanish (i.e., there are simultaneously nonzero electric- and magnetic-dipole transition moments in the $|2\rangle$-$|-\rangle$ transition process). Hence, both electric- and magnetic-dipole allowed transitions between the bare level $|2\rangle$ and the mixed-parity dressed level $|-\rangle$ will occur, if the level pair $|2\rangle$-$|-\rangle$ is coupled to the electric and magnetic fields of an incident probe beam.

Now the mixed-parity atomic dressed state $|-\rangle$ makes the atomic electric- and magnetic-dipole moments (due to $|2\rangle$-$|-\rangle$ transition) simultaneously nonzero, and the microscopic electric and magnetic polarizabilities $\beta_{\rm e}$, $\beta_{\rm m}$ of atoms have almost the same optically resonant behavior, e.g., both $\beta_{\rm e}$ and $\beta_{\rm m}$ are determined by the same density matrix element $\rho_{-,2}$ (to be shown in Eq. (5)). In other words, the resonance frequencies of the electric permittivity and the magnetic permeability would be in the same ranges (or the resonance frequency ranges of permittivity and permeability are overlapped). This means that the simultaneously negative permittivity and permeability could be realized in the same frequency bands. This will be demonstrated in more details in Section 3 (the theoretical model) and in Section 4 (a numerical example).

3. DENSITY MATRIX EQUATION OF THE INCOHERENT-GAIN DRESSED-STATE SYSTEM

We shall now consider the optical behavior of the present system involving the incoherent-gain dressed-state transitions. According to the Schrödinger equation, the equation of motion of the density matrix of the atomic system in Fig. 1 is given by

$$\begin{aligned}
\dot{\rho}_{11} &= -\lambda\rho_{11} + \gamma_{-1}\rho_{--} + \gamma_{21}\rho_{22}, \\
\dot{\rho}_{22} &= -\gamma_{21}\rho_{22} + \gamma_{-,2}\rho_{--} - \frac{\mathrm{i}}{2}\Omega\rho_{2-} + \frac{\mathrm{i}}{2}\Omega^*\rho_{-,2}, \\
\dot{\rho}_{--} &= \lambda\rho_{11} - (\gamma_{-,1} + \gamma_{-,2})\,\rho_{--} + \frac{\mathrm{i}}{2}\Omega\rho_{2-} - \frac{\mathrm{i}}{2}\Omega^*\rho_{-,2}, \\
\dot{\rho}_{-,2} &= -(\gamma + \mathrm{i}\Delta)\,\rho_{-,2} + \frac{\mathrm{i}}{2}\Omega\,(\rho_{22} - \rho_{--})\,, \\
\dot{\rho}_{2-} &= -(\gamma - \mathrm{i}\Delta)\,\rho_{2-} - \frac{\mathrm{i}}{2}\Omega^*\,(\rho_{22} - \rho_{--})\,,
\end{aligned} \tag{4}$$

where the probe frequency detuning $\Delta = \omega_{-,2} - \omega_{\mathrm{p}}$ with $\omega_{-,2}$ the transition frequency between the dressed level $|-\rangle$ and the bare level $|2\rangle$, λ denotes the pumping rate of the population from the ground level $|1\rangle$ to the dressed level $|-\rangle$, and $\Omega = \Omega_{\mathrm{E}} + \Omega_{\mathrm{B}}$ with the electric Rabi frequency $\Omega_{\mathrm{E}} = p_{-,2}\mathcal{E}_{\mathrm{p}}/\hbar$ and the magnetic Rabi frequency $\Omega_{\mathrm{B}} = m_{-,2}\mathcal{B}_{\mathrm{p}}/\hbar$. The decay rate γ is defined as $\gamma = (\gamma_{-,1} + \gamma_{-,2} + \gamma_{21} + \gamma_{\mathrm{ph}})/2$. The diagonal density matrix elements ρ_{11}, ρ_{22}, and ρ_{--} agree with a constraint of probability (population) conservation, i.e., $\rho_{11} + \rho_{22} + \rho_{--} = 1$. It should be emphasized that the density matrix elements ρ_{21}, $\rho_{-,1}$, $\rho_{+,1}$, ρ_{+-}, $\rho_{+,2}$ and ρ_{++} that are not taken into account in Eq. (4) will decay exponentially to zero (i.e., $\rho_{ij} = \rho_{ij}^{(0)}\mathrm{e}^{-\Gamma_{ij}t} \to 0$), i.e., their steady solutions are $\rho_{21} = 0$, $\rho_{-,1} = 0$, $\rho_{+,1} = 0$, $\rho_{+-} = 0$, $\rho_{+,2} = 0$, and $\rho_{++} = 0$.

We shall demonstrate the optical left handedness of the pumped atomic vapor. The steady solution of Eq. (4) is particularly essential for this purpose. The expressions for the microscopic electric and magnetic polarizabilities of the atom are given by $\beta_{\mathrm{e}} = 2p_{2-}\rho_{-,2}/(\varepsilon_0\mathcal{E}_{\mathrm{p}})$, $\beta_{\mathrm{m}} = 2\mu_0 m_{2-}\rho_{-,2}/\mathcal{B}_{\mathrm{p}}$, which can also be rewritten as

$$\beta_{\mathrm{e}} = \frac{2|p_{-,2}|^2}{\varepsilon_0\hbar\Omega_{\mathrm{E}}}\rho_{-,2}, \qquad \beta_{\mathrm{m}} = \frac{2\mu_0|m_{-,2}|^2}{\hbar\Omega_{\mathrm{B}}}\rho_{-,2}, \tag{5}$$

if the expressions for the electric Rabi frequency $\Omega_{\mathrm{E}} = p_{-,2}\mathcal{E}_{\mathrm{p}}/\hbar$ and the magnetic Rabi frequency $\Omega_{\mathrm{B}} = m_{-,2}\mathcal{B}_{\mathrm{p}}/\hbar$ are taken into consideration. Here, the scalars $p_{-,2}$ and $m_{-,2}$ are the magnitudes of the electric dipole moment vector $\mathbf{p}_{-,2}$ and the magnetic dipole moment vector $\mathbf{m}_{-,2}$, respectively. In order to achieve the negative permittivity and

the negative permeability, the chosen vapor should be dense, so that one should consider the local field effect, i.e., one must distinguish between the applied macroscopic fields and the microscopic local fields that act upon the atoms in the vapor when addressing how the atomic transitions are related to the electric and magnetic susceptibilities [32]. The electric and magnetic Clausius-Mossotti relations [32, 33] that can reveal the connection between the macroscopic quantities ($\varepsilon_{\rm r}$ and $\mu_{\rm r}$) and the microscopic polarizabilities ($\beta_{\rm e}$ and $\beta_{\rm m}$) are of the form $\varepsilon_{\rm r} = (1+\frac{2}{3}N\beta_{\rm e})/(1-\frac{1}{3}N\beta_{\rm e})$ and $\mu_{\rm r} = (1+\frac{2}{3}N\beta_{\rm m})/(1-\frac{1}{3}N\beta_{\rm m})$, respectively, where N denotes the atomic concentration (total number of atoms per unit volume) of the atomic vapor [32, 33].

4. A NUMERICAL EXAMPLE FOR SIMULTANEOUSLY NEGATIVE PERMITTIVITY AND PERMEABILITY

The three-dimensionally isotropic negative refractive index of the quantum-coherent atomic vapor is expected to occur under proper conditions, which will be demonstrated in our numerical example. We choose the electric- and magnetic-dipole transition moments for the present system as $p_{a2} = 1.0\times10^{-29}\,{\rm C\cdot m}$ (pure-parity transition dipole moment induced in the transition $|2\rangle$-$|a\rangle$) and $m_{b2} = 5.5\times10^{-23}\,{\rm C\cdot m^2\cdot s^{-1}}$ (pure-parity transition dipole moment induced in the transition $|2\rangle$-$|b\rangle$), respectively. The typical values for the decay rates due to spontaneous emission are $\gamma_{-,1} = 3.0\times10^{6}\,{\rm s^{-1}}$, $\gamma_{-,2} = 1.0\times10^{4}\,{\rm s^{-1}}$, $\gamma_{21} = 1.5\times10^{6}\,{\rm s^{-1}}$, and the collisional dephasing rate of atoms $\gamma_{\rm ph} = 1.0\times10^{6}\,{\rm s^{-1}}$. Then the normalized parameter γ (defined as $\gamma \equiv (\gamma_{-,1}+\gamma_{-,2}+\gamma_{21}+\gamma_{\rm ph})/2$) that will appear in Δ/γ in the following figures is $2.8\times10^{6}\,{\rm s^{-1}}$. The number density of atoms is $N = 1.2\times10^{24}$ Atoms ${\rm m^{-3}}$. The pumping rate $\lambda = 9.0\times10^{6}\,{\rm s^{-1}}$. All these (atomic and optical) parameters will be adopted throughout this work.

The electric Rabi frequency of the incident probe field is chosen as $\Omega_{\rm E} = 5.0\times10^{6}\,{\rm s^{-1}}$, and the magnetic Rabi frequency $\Omega_{\rm B} = \frac{m_{-,2}}{cp_{-,2}}\Omega_{\rm E}$, which is $3.0\times10^{6}\,{\rm s^{-1}}$ (corresponding to the dressed-state mixing angle $\vartheta = -0.03$) and $2.3\times10^{6}\,{\rm s^{-1}}$ (corresponding to the dressed-state mixing angle $\vartheta = -0.04$). Both the real and the imaginary parts of the relative permittivity $\varepsilon_{\rm r}$, the relative permeability $\mu_{\rm r}$, the refractive index n and the relative impedance $\eta_{\rm r}$ are shown in Fig. 2, where two cases corresponding to the dressed-state mixing angle $\vartheta = -0.03$ and $\vartheta = -0.04$ are given as an illustrative example. It can be found that, in the case of $\vartheta = -0.03$, the real part of the permittivity, ${\rm Re}\varepsilon_{\rm r}$, is negative in the range $[-15.7\gamma, 0.0\gamma]$ of the frequency detuning Δ,

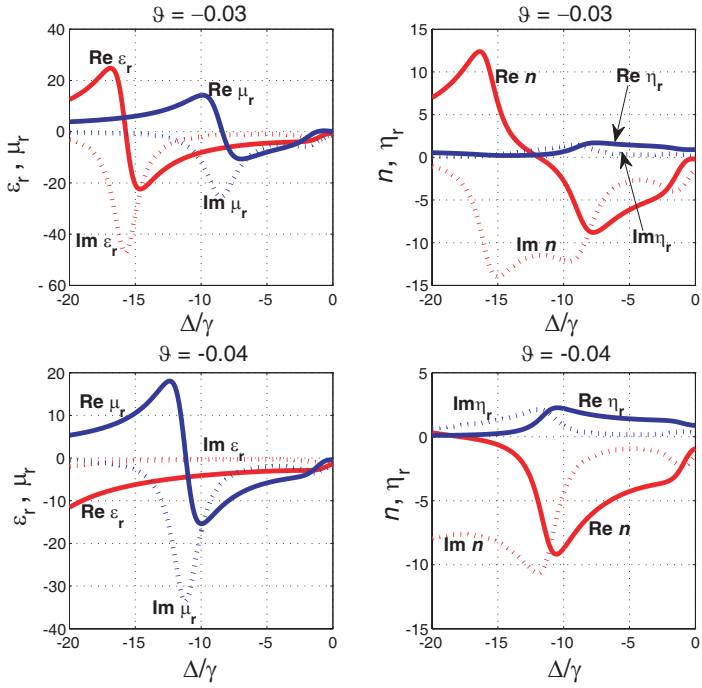

Figure 2. The dispersion characteristics of the relative permittivity $\varepsilon_{\rm r}$, the relative permeability $\mu_{\rm r}$, the relative impedance $\eta_{\rm r}$ and the refractive index n of the atomic vapor driven by the incoherent pump field (for high-gain amplification) and the strong coupling field (for generating dressed states). The electric Rabi frequency of the incident probe field is chosen as $\Omega_{\rm E} = 5.0 \times 10^6\,{\rm s}^{-1}$.

and the real part of the permeability, Re$\mu_{\rm r}$, is negative in the range $[-8.5\gamma, -1.0\gamma]$ of the frequency detuning Δ. In all the frequency ranges of interest shown in Fig. 2, the imaginary parts of both $\varepsilon_{\rm r}$ and $\mu_{\rm r}$ are always negative. It can also be seen that the real part, Ren, of the refractive index is negative when the frequency detuning Δ is in the range $[-12.0\gamma, 0.0\gamma]$, where the imaginary part, Imn, is also negative (due to incoherent gain by the incoherent pump field). The minimum value of the real part Ren is -8.8 at the position $\Delta = -7.6\gamma$. For the case of $\vartheta = -0.04$, the real part of the permittivity, Re$\varepsilon_{\rm r}$, is always negative in the frequency detuning range as shown in Fig. 2, and the real part of the permeability, Re$\mu_{\rm r}$, is negative in the range $[-11.0\gamma, 0.0\gamma]$ of the frequency detuning. Besides, the imaginary parts of both $\varepsilon_{\rm r}$ and $\mu_{\rm r}$ are negative in these frequency detuning bands. Then the imaginary part of the refractive index is also negative (because of incoherent gain), and the refractive index n has a negative real part in

the frequency detuning range $[-18.0\gamma, 0.0\gamma]$ with its minimum value $\mathrm{Re}n = -9.2$ at the position $\Delta = -10.5\gamma$.

The tunable dispersion characteristics of both the real and the imaginary parts of the refractive index n and the relative impedance η_{r} of the left-handed atomic vapor are shown in Fig. 3. Here, the dressed-state mixing angle ϑ changes (caused by the tunable Rabi frequency Ω_{c} of the strong coupling field. In the schematic diagram in Fig. 1, this strong coupling field couples the bare levels $|a\rangle$ and $|b\rangle$, and this leads to two dressed states $|\pm\rangle$). It can be seen that the real part of the refractive index of the present quantum-coherent double-negative atomic medium is negative when the dressed-state mixing angle ϑ increases (i.e., the intensity of the coupling field Ω_{c} becomes stronger). It can also be found that the imaginary part of the refractive index is always negative in the parameter ranges of both Δ/γ and ϑ shown in Fig. 3. Since the imaginary part and the real part of the refractive index have the same order of magnitude, this would lead to high gain optical amplification of an electromagnetic wave propagating inside the present left-handed atomic vapor. This may be viewed as a new route to low-loss, lossless, and active negative refracting materials.

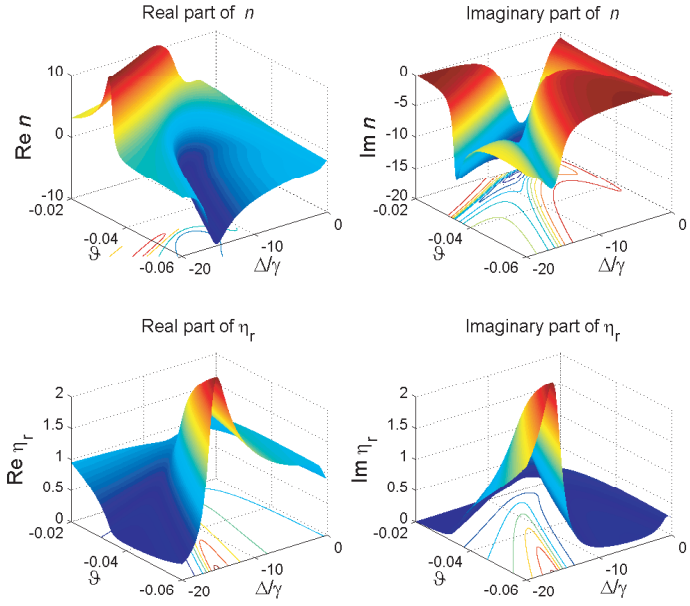

Figure 3. The tunable behavior of dispersion of the real and imaginary parts of the refractive index n and the relative impedance η_{r}.

5. DISCUSSIONS OF THE NEGATIVE INDICES DEPENDING UPON THE PROBE BEAM INTENSITY

In the preceding section, we have shown that there is double-negative left handedness in optical wave propagating inside the present atomic vapor under certain proper parameter conditions. In Figs. 2 and 3, the frequency detuning Δ is in the range $[-20\gamma, 0]$, where both the real and the imaginary parts of $\varepsilon_{\rm r}$, $\mu_{\rm r}$ and n are quite negative (e.g., in the range $[-10, 0]$). In this section, we shall consider the other frequency detuning range $[0, 40\gamma]$, in which both the real and the imaginary parts of $\varepsilon_{\rm r}$, $\mu_{\rm r}$ and n are negative but in a relatively narrow range (e.g., $[-2, 0]$). In Fig. 4 we present the dispersion characteristics of the relative permittivity $\varepsilon_{\rm r}$, the relative permeability $\mu_{\rm r}$, the relative impedance $\eta_{\rm r}$ and the refractive index n of the atomic vapor with incoherent gain. All the atomic and optical parameters are exactly the same as those in Fig. 2. Take the case of the dressed-state mixing angle $\vartheta = -0.03$ as an example. It can be found in Fig. 4 that ${\rm Re}\varepsilon_{\rm r} = -0.60$ when the frequency detuning $\Delta = 0.0\gamma$, and ${\rm Re}\varepsilon_{\rm r} = 0.0$ when the frequency detuning $\Delta = 33.0\gamma$ (i.e., ${\rm Re}\varepsilon_{\rm r}$ is always negative in the frequency detuning range $[0.0, 33.0\gamma]$). The minimum of ${\rm Re}\varepsilon_{\rm r}$ is -1.1 at $\Delta = 4.1\gamma$. The real part of $\mu_{\rm r}$ is 0.0 when $\Delta = 0.20\gamma$ and 19.5γ (i.e., ${\rm Re}\mu_{\rm r}$ is always negative in the frequency detuning range $[0.20\gamma, 19.5\gamma]$). The minimum of ${\rm Re}\mu_{\rm r}$ is -0.72 at the frequency detuning $\Delta = 3.7\gamma$. Therefore, in the frequency detuning band $[0.20\gamma, 19.5\gamma]$, both ${\rm Re}\varepsilon_{\rm r}$ and ${\rm Re}\mu_{\rm r}$ are simultaneously negative. In all these frequency ranges, the imaginary parts of both $\varepsilon_{\rm r}$ and $\mu_{\rm r}$ are negative, e.g., their values are in the range $[-1.5, 0.0]$. For $\vartheta = -0.03$, it can also be found from Fig. 4 that the real part ${\rm Re}n$ of the refractive index is -0.29 at $\Delta = 0.20\gamma$, where the real part ${\rm Re}\mu_{\rm r} = 0.0$, and ${\rm Re}n = -0.11$ at $\Delta = 19.5\gamma$, where the real part ${\rm Re}\mu_{\rm r}$ is also 0.0. The minimum of ${\rm Re}n$ is -0.88 when $\Delta = 3.6\gamma$. The imaginary part ${\rm Im}n$ of the refractive index is -1.2 at $\Delta = 0.20\gamma$ and ${\rm Im}n = -6.3 \times 10^{-2}$ at $\Delta = 19.5\gamma$. The maximum of ${\rm Im}n$ is ${\rm Im}n = -5.5 \times 10^{-2}$ when $\Delta = 16.4\gamma$.

Since the amplification factor of the wave across a single wavelength at, e.g., $\Delta = 16.4\gamma$, is $\exp(2\pi \times 5.5 \times 10^{-2}) = 1.4$, we should, however, emphasize that the present negative refractive index with a quite negative imaginary part is in fact unstable, i.e., such a large amount of gain will spoil the negative-index effect. To clarify this point, we illustrate the dispersion behavior of $\varepsilon_{\rm r}$, $\mu_{\rm r}$, $\eta_{\rm r}$ and n in Fig. 5 when the incident probe field (characterized by the Rabi frequency $\Omega_{\rm E}$) is amplified. The electric Rabi frequency is chosen as $\Omega_{\rm E} = 3.0 \times 10^7\,{\rm s}^{-1}$, and the magnetic Rabi frequency $\Omega_{\rm B} = 1.8 \times 10^7\,{\rm s}^{-1}$ (corresponding to the dressed-state mixing angle $\vartheta = -0.03$) and $1.4 \times 10^7\,{\rm s}^{-1}$

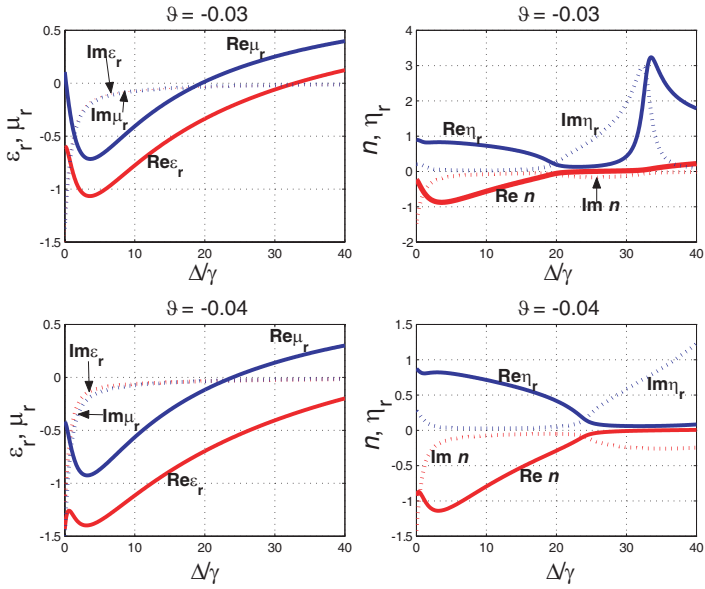

Figure 4. The dispersion characteristics of the relative permittivity $\varepsilon_{\rm r}$, the relative permeability $\mu_{\rm r}$, the relative impedance $\eta_{\rm r}$ and the refractive index n of the atomic vapor with incoherent gain. All the atomic and optical parameters are chosen exactly the same as those in Fig. 2.

(corresponding to the dressed-state mixing angle $\vartheta = -0.04$). It can be seen that the real parts of $\varepsilon_{\rm r}$ and $\mu_{\rm r}$ in the case of $\vartheta = -0.03$ are no longer negative when the Rabi frequency $\Omega_{\rm E}$ has the order of a few $10^7\,{\rm s}^{-1}$. Thus, the present dressed-state assisted negative-index medium is unstable for achieving negative indices and would be no longer essentially important for practical applications when the propagating beam is amplified to the order of magnitude of $10^7\,{\rm s}^{-1}$ (in its Rabi frequency).

In the above, we have shown the existence of double-negative left handedness in the atomic vapor for optical wave propagation when the intensity (or the Rabi frequency) is large (e.g., $\Omega_{\rm E} \simeq 10^6 \sim 10^7\,{\rm s}^{-1}$). It can be found that the dispersion behavior of $\varepsilon_{\rm r}$, $\mu_{\rm r}$, $\eta_{\rm r}$ and n (when the incident wave is weak, e.g., $\Omega_{\rm E} = 5.0 \times 10^2\,{\rm s}^{-1}$ shown in Fig. 6) is somewhat similar to that of $\Omega_{\rm E} = 5.0 \times 10^6\,{\rm s}^{-1}$ shown in Fig. 4, namely, the optical response of the present negative-index atomic vapor in the frequency detuning range $[0, 40\gamma]$ is not sensitive to the intensity of the amplified propagating wave. Only when the Rabi frequency $\Omega_{\rm E} \gg 5.0 \times 10^6\,{\rm s}^{-1}$ will the negative-index atomic vapor exhibits its

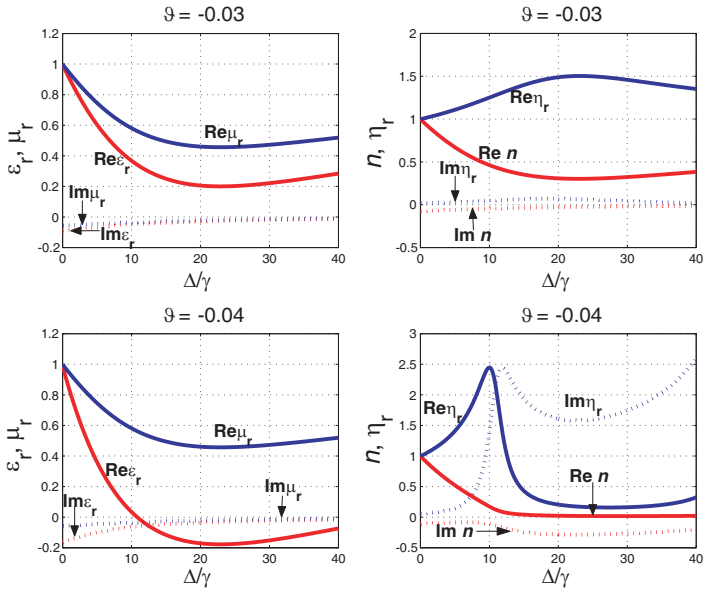

Figure 5. The dispersion characteristics of the relative permittivity $\varepsilon_{\rm r}$, the relative permeability $\mu_{\rm r}$, the relative impedance $\eta_{\rm r}$ and the refractive index n of the atomic vapor when the incident probe field becomes strong. The electric Rabi frequency of the incident probe field is chosen as $\Omega_{\rm E} = 3.0 \times 10^7\,{\rm s}^{-1}$.

optical nonlinearity (i.e., sensitive to the intensity of the amplified propagating wave), and the negative indices will no longer be present (see Fig. 5). If the initial Rabi frequency of the incident weak light is $\Omega_{\rm E} = 5.0 \times 10^2\,{\rm s}^{-1}$, then according to the negative Imn value, e.g., Im$n = -5.5 \times 10^{-2}$ at $\Delta = 16.4\gamma$ (in the case of $\vartheta = -0.03$ in Fig. 4), the incident weak light will be amplified to $\Omega_{\rm E} = 5.0 \times 10^6\,{\rm s}^{-1}$ after it propagates across 27 wavelengths (i.e., $\frac{\ln 10^4}{2\pi \times 5.5 \times 10^{-2}} \simeq 27$). This means that at least 27 wavelengths can the wave propagate in the present negative-index atomic medium before it can be absorbed.

6. SOME PROBLEMS IN EXPERIMENTAL VERIFICATION OF DOUBLE-NEGATIVE LEFT-HANDED ATOMIC VAPOR

We will discuss some problems such as number density of atoms, laser beam intensity required in the left-handed atomic vapor, and its negative refraction verification in experiments.

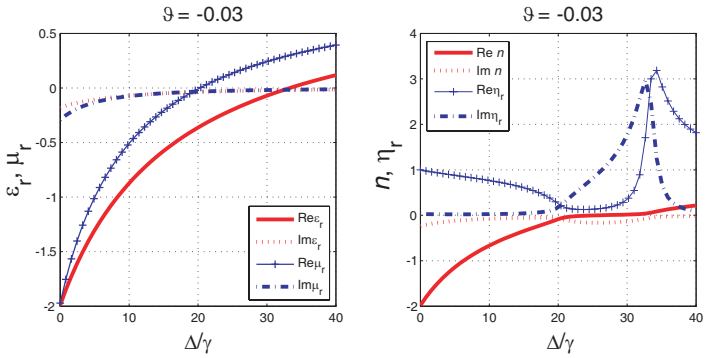

Figure 6. The dispersion characteristics of the relative permittivity $\varepsilon_{\rm r}$, the relative permeability $\mu_{\rm r}$, the relative impedance $\eta_{\rm r}$ and the refractive index n of the atomic vapor when the incident probe field is weak, i.e., the electric Rabi frequency of the incident probe field is chosen as $\Omega_{\rm E} = 5.0 \times 10^2\,{\rm s}^{-1}$.

In the preceding sections, we have shown that the required atomic vapor for double-negative left handedness is dense in its number density (total number of atoms per unit volume). In general, the dilute alkali-metal atomic vapors have the number density with the order of magnitude of $10^{19} \sim 10^{20}$ Atoms m^{-3} at room temperature (e.g., 300 K) [34–37]. The number density will increase when the atomic vapor cell is heated to a high temperature. According to the thermodynamic statistics, the number density N of a saturated atomic vapor is given by [38]

$$N = N_0 \frac{T_0}{T} \exp\left[-\frac{l}{k_{\rm B}}\left(\frac{1}{T} - \frac{1}{T_0}\right)\right], \tag{6}$$

where N_0 is the number density at a certain temperature T_0, l the sublimation energy per atom, and $k_{\rm B}$ the Boltzmann constant. The typical parameters can be chosen as follows: $N_0 = 10^{19}$ Atoms m^{-3} at $T_0 = 300$ K, and the sublimation energy per atom is 1.0×10^{-19} J/atom. In order to obtain the density $N = 1.2 \times 10^{24}$ Atoms m^{-3} that is required for realizing a double-negative left-handed atomic vapor, the absolute temperature of the atomic vapor should be $T \simeq \frac{1}{\frac{1}{T_0} - \frac{k_{\rm B}}{l} \ln \frac{N}{N_0}} \simeq$ 573 K. Since quantum coherent effects in atomic vapors at temperature 300 K to 1000 K have been demonstrated experimentally [34–40], we believe that the present atomic vapor with density $N = 1.2 \times 10^{24}$ Atoms m^{-3} could also be achieved experimentally.

We shall here evaluate the power (intensity) of the laser beam sources. The power of the driving beam required can be obtained

with the commercial sources. Such beam sources have been utilized in previous experiments of quantum coherence (e.g., electromagnetically induced transparency) in various atomic vapor media [41–44]. In Figs. 2 and 4, the electric Rabi frequency of the incident probe field is chosen as $\Omega_{\rm E} = 5.0 \times 10^6\,{\rm s}^{-1}$. Since the electric Rabi frequency is defined as $\Omega_{\rm E} = p_{-,2}\mathcal{E}_{\rm p}/\hbar$, where $p_{-,2}$ has the magnitude $1.0 \times 10^{-29}|\sin\vartheta|\,{\rm C}\cdot{\rm m}$, e.g., Eq. (3), the electric field strength of the applied beam is $\mathcal{E}_{\rm p} = \frac{\hbar\Omega_{\rm E}}{1.0\times10^{-29}|\sin\vartheta|}$ (in SI units). In the reference of experiments of atomic phase coherence [41], the Rabi frequency $\Omega'_{\rm E} = 2\pi \times 90 \times 10^6\,{\rm s}^{-1}$ corresponds to the laser intensity $250\,{\rm W/cm}^2$ (at the beam waist). Here, the electric dipole moment of atoms has the order of magnitude of $1.0\times10^{-29}\,{\rm C}\cdot{\rm m}$. Then the electric field strength in Ref. [41] is $\mathcal{E}'_{\rm p} \simeq \frac{\hbar\Omega'_{\rm E}}{1.0\times10^{-29}}$ (in SI units). Thus, the laser beam intensity in the present scheme of atomic-vapor negative refraction is $250\left(\frac{\Omega_{\rm E}}{\Omega'_{\rm E}|\sin\vartheta|}\right)^2 \simeq 22\,{\rm W/cm}^2$, where, as an illustrative example, we have chosen the dressed-state mixing parameter $|\sin\vartheta| \simeq |\vartheta| = 0.03$ (see Figs. 2 and 4).

The negative refractive index of the atomic vapor presented in the paper is achieved based on the mixed-parity dressed-state assisted resonance as well as quantum coherence (atomic phase coherence). In the literature, over the past two decades, there have been a number of experiments of quantum coherence, including various quantum interference effects relevant to electromagnetically induced transparency (EIT) in atomic vapors [41–44]. The optical response of dressed-state atomic vapor has also been observed [43]. Thus, we believe that the experimental realization of the present dressed-state assisted negative refractive index can in principle be demonstrated by the commercial devices available for quantum coherence (atomic phase coherence) [41–44].

Now we shall discuss briefly the problem of experimental demonstration of double-negative left-handed atomic vapor. Left-handed media can exhibit many unusual electromagnetic and optical effects such as negative refraction [45], negative Goos-Hänchen effect [10], reversed Doppler effect and negative Cerenkov radiation caused by the negative refractive index [46]. These effects can be used to demonstrate the existence of double-negative left handedness (and hence the corresponding negative refractive index). Here, we address the problem of the possible experimental verification of double-negative left handedness in an atomic vapor by using the effects of negative refraction and Goos-Hänchen lateral shift: *i*) The atoms such as neutral alkali-metal atoms (e.g., the neutral rubidium or cesium atoms) can be stored in an atomic vapor cell [41]. An incident wave strikes the

atomic vapor cell, giving rise to a reflected wave and a refracted wave. If the atomic vapor has negative refractive index, then the anomalous refraction effect for the transmitted wave into the atomic vapor will occur. Measurements of such phenomena of negative refraction in solid materials have been performed in many experiments of left-handed materials [47–50]. *ii*) As is well known, in an ordinary Goos-Hänchen shift effect (where a wave is incident from one positive-refractive-index medium into another positive-refractive-index medium), the totally reflected beam experiences a lateral displacement from its position on the interface, since each of the plane wave components of the incident wave striking the interface undergoes their respective phase change in this reflection process [10]. If the wave is incident into a left-handed medium and then reflected, the lateral displacement, which is opposite to that in the ordinary Goos-Hänchen effect, will result from the negativity in the refractive index. Then one can demonstrate the atomic-vapor negative refraction by taking advantage of such a negative Goos-Hänchen shift effect [10, 51–53].

7. AN APPLICATION FOR SURFACE PLASMON WAVE

We have shown theoretically how to realize a three-dimensionally isotropic double-negative atomic vapor based on quantum optical mechanism. It should be pointed out that a single negative medium (i.e., either $\varepsilon_{\rm r}$ or $\mu_{\rm r}$ is negative), which can exhibit some new attractive optical responses, can also be achieved with the present mechanism. If, for example, the strong coupling field, which drives the $|b\rangle$-$|a\rangle$ transition and leads to two orthogonal dressed states $|\pm\rangle$, is switched off (i.e., the Rabi frequency $\Omega_{\rm c} = 0$ and hence the dressed-state mixing angle $\vartheta = 0$), the present atomic vapor will become a single negative-$\mu_{\rm r}$ medium, of which the dispersion characteristics of both the real and the imaginary parts of the relative permeability $\mu_{\rm r}$ and the refractive index n are plotted in Fig. 7. Here, the magnetic Rabi frequency is chosen as $\Omega_{\rm B} = 3.0 \times 10^6\,{\rm s}^{-1}$. It can be found that the real part of $\mu_{\rm r}$ is negative when the frequency detuning Δ is in the range $[-3.1\gamma, 6.0\gamma]$ with the minimum value ${\rm Re}\mu_{\rm r} = -2.9$ at $\Delta = -2.1\gamma$ and the corresponding imaginary part ${\rm Im}\mu_{\rm r} = -5.7$. Since there is no coupling field, the two dressed states $|\pm\rangle$ are no long present, and the probe field only drives the $|2\rangle$-$|b\rangle$ magnetic-dipole allowed transition, instead of the $|2\rangle$-$|-\rangle$ mixed-parity transition. Thus, the relative permittivity of the present atomic medium is 1. Such a negative-permeability atomic medium can be utilized to sustain a TE-mode surface plasmon wave at its interface adjacent to a dielectric of $\mu_{\rm r} = 1$. If, for example, the permeability of the negative-permeability atomic medium has a sufficiently negative

real part, then a surface plasmon wave (excited by external power stimuli) can propagate in the direction parallel to the interface. But in the direction perpendicular to the interface, it decays evanescently on both sides of the interface. The magnetic field distribution of the surface plasmon wave when $\mu_{\rm r} = -2.9 - 5.7{\rm i}$ (i.e., the permeability has its minimum value in its real part as shown in Fig. 7) is depicted in Fig. 8, where a single, flat interface between the negative-permeability atomic medium and the dielectric of $\mu_{\rm r} = 1$ is in the $\hat{y}$-$\hat{z}$ plane of a Cartesian coordinate system. It can be seen that the surface plasmon wave amplitude exponentially decays in the $\hat{x}$-direction (perpendicular to the interface). In the $\hat{z}$-direction (parallel to the interface), however, the complex propagation constant has a negative imaginary part and hence the field strength of the surface wave can be amplified.

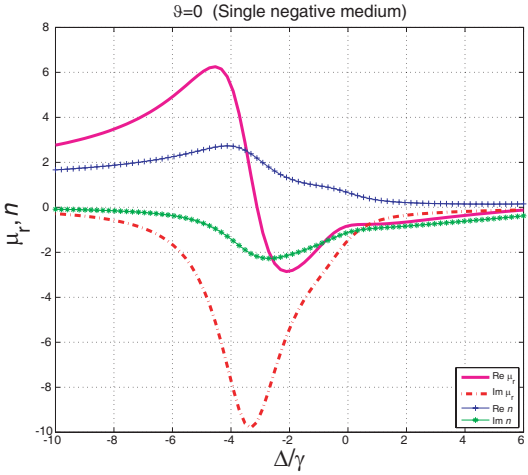

Figure 7. The real and imaginary parts of the relative permeability $\mu_{\rm r}$ and the refractive index n when the strong coupling field is switched off (i.e., the Rabi frequency $\Omega_{\rm c} = 0$ and hence the dressed-state mixing angle $\vartheta = 0$).

In general, the electromagnetic surface plasmon excitation generated in metal-based structures is in high frequency bands. The present scheme can, however, be used to realize surface plasmon resonance in terahertz band. If, for example, we choose the atomic system $\{|1\rangle, |2\rangle, |b\rangle, |a\rangle\}$ in Fig. 1 as the neutral sodium atomic system $\{3^2{\rm S}_{\frac{1}{2}}, 3^2{\rm P}_{\frac{1}{2}}, 3^2{\rm P}_{\frac{3}{2}}, 4^2{\rm S}_{\frac{1}{2}}\}$ with its energy levels $\{0.000, 16956.172, 16973.368, 25739.991\}\,{\rm cm}^{-1}$ [54], where the transition frequency between level $3^2{\rm P}_{\frac{1}{2}}$ and level $3^2{\rm P}_{\frac{3}{2}}$ is $3.2\times10^{12}\,{\rm s}^{-1}$

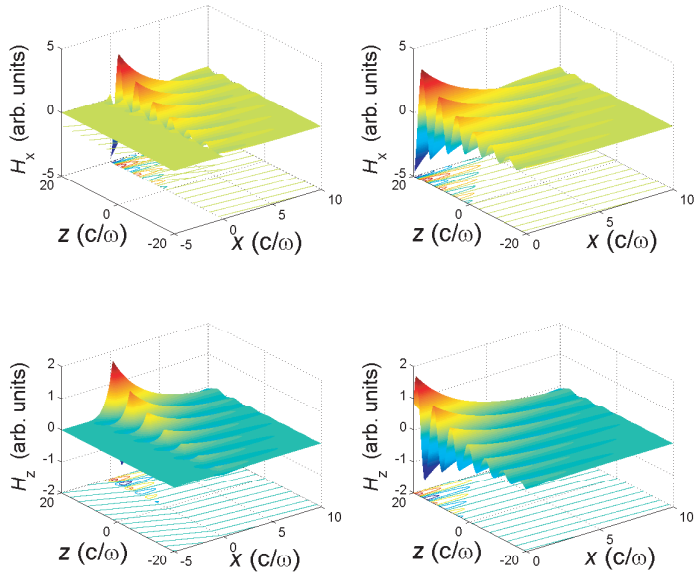

Figure 8. The spatial field profile of a TE-mode surface plasmon wave at the interface between the dielectric of $\mu_r = 1$ and the single negative atomic medium. The negative-permeability atomic medium is in the half space $x < 0$ and the dielectric in the other half space $x > 0$.

(angular frequency), then such an atomic medium will have a negative permeability in terahertz band. In addition, the surface plasmon wave excited with such a medium is extremely sensitive to dispersion, since in the negative permeability, the frequency appears as $1/(\omega_{ij} - \omega)$ (rather than as $1/\omega$ as shown in the Lorentz-model media). Therefore, the dispersion in the atomic medium is quite large, e.g., 10^8 times that in metal. The dispersion-sensitive surface plasmon wave would have potential applications in design of new optical sensors and modulators. Since the permittivity and permeability can be quantum-coherently controlled by the strong coupling field, the tunable surface plasmon wave modes can exhibit controllable optical responses driven by the external optical fields.

In a word, the surface plasmon wave presented here may have four attractive features: *i*) surface plasmon wave amplification by an incoherent pumping field; *ii*) surface plasmon wave at terahertz frequencies; *iii*) surface plasmon wave sensitive to dispersion; *iv*) surface plasmon wave controllably manipulated by external optical fields.

8. CONCLUDING REMARKS

The simultaneous electric- and magnetic-dipole optical responses of atomic transitions are excited by a probe wave with both *dressed-state assisted mixed-parity transitions* and *incoherent population transfer*. This can give rise to a three-dimensionally isotropic and homogeneous negative refractive index. Here, the dressed-state assisted transitions enable to realize simultaneously negative permittivity and permeability in the same frequency bands. In the previous references [17–22], loss of left-handed atomic vapor based on quantum coherence was in general quite large, and this would make such negatively refracting atomic media not realistic in practical applications. Here, we have suggested a new mechanism of incoherent population transfer, where a pumping action is involved for achieving high-gain optical amplification in the negative-index quantum-coherent atomic vapor. Such a scheme of negative refraction has some advantages, e.g., *three-dimensionally isotropic* double-negative indices *at visible and infrared wavelengths*. This can lead to *quantum-coherent tunable* negative refractive index and *loss-free or active* optical response of the atomic medium via *incoherent high-gain optical amplification*. We expect that it could be experimentally realized in the near future. Such scenarios of three-dimensionally isotropic optical left handedness and high-gain optical amplification would have potential applications in designs of new quantum optical and photonic devices, including particularly subwavelength focusing system and negative-index superlenses for perfect imaging [4].

ACKNOWLEDGMENT

This work is supported in part by the National Natural Science Foundation of China under Grants Nos. 11174250, 91233119 and 60990320.

REFERENCES

1. Shelby, R. A., D. R. Smith, and S. Schultz, "Experimental verification of a negative index of refraction," *Science*, Vol. 292, 77–79, 2001.
2. Pendry, J. B., A. J. Holden, W. J. Stewart, and I. Youngs, "Extremely low frequency plasmons in metallic mesostructures," *Phys. Rev. Lett.*, Vol. 76, 4773–4776, 1996.
3. Pendry, J. B., A. J. Holden, D. J. Robbins, and W. J. Stewart,

"Low frequency plasmons in thin wire structures," *J. Phys. Condens. Matter*, Vol. 10, 4785–4809, 1998.

4. Pendry, J. B., "Negative refraction makes a perfect lens," *Phys. Rev. Lett.*, Vol. 85, 3966–3969, 2001.
5. Zheludev, N. I., S. L. Prosvirnin, N. Papasimakis, and V. A. Fedotov, "Lasing spaser," *Nat. Photon.*, Vol. 2, 351–354, 2008.
6. Poutrina, E., D. Huang, and D. R. Smith, "Analysis of nonlinear electromagnetic metamaterials," *New J. Phys.*, Vol. 12, 093010, 2010.
7. Xiao, S., V. P. Drachev, A. V. Kildishev, X. Ni, U. K. Chettiar, H.-K. Yuan, and V. M. Shalaev, "Loss-free and active optical negative-index metamaterials," *Nature*, Vol. 466, 735–738, 2010.
8. Liu, N., M. Hentschel, T. Weiss, A. P. Alivisatos, and H. Giessen, "Three-dimensional plasmon rulers," *Science*, Vol. 332, 1407–1410, 2011.
9. Weis, P., J. L. Garcia-Pomar, R. Beigang, and M. Rahm, "Hybridization induced transparency in composites of metamaterials and atomic media," *Opt. Express*, Vol. 19, 23573–23580, 2011.
10. Dong, W., L. Gao, and C.-W. Qiu, "Goos-Hänchen shift at the surface of chiral negative refractive media," *Progress In Electromagnetics Research*, Vol. 90, 255–268, 2009.
11. Koschny, Th., L. Zhang, and C. M. Soukoulis, "Isotropic three-dimensional left- handed metamaterials," *Phys. Rev. B*, Vol. 71, 121103-R, 2005.
12. Vendik, I., O. Vendik, and M. Odit, "Isotropic artificial media with simultaneously negative permittivity and permeability," *Microwave Opt. Techn. Lett.*, Vol. 18, 2553–2556, 2006.
13. Guney, D. O., T. Koschny, and C. M. Soukoulis, "Intra-connected three-dimensionally isotropic bulk negative index photonic metamaterial," *Opt. Express*, Vol. 18, 12348–12353, 2010.
14. Logeeswaran, V. J., M. S. Islam, M. L. Chan, D. A. Horsley, W. Wu, S.-Y. Wang, and R. S. Williams, "Realization of 3D isotropic negative index materials using massively parallel and manufacturable microfabrication and micromachining technology," *Mater. Res. Soc. Symp. Proc.*, Vol. 919, 0919-J02-01, 2006.
15. Hu, L. B. and S. T. Chui, "Characteristics of electromagnetic wave propagation in uniaxially anisotropic left-handed materials," *Phys. Rev. B*, Vol. 66, 085108, 2002.

16. Choi, J. and C. Seo, "High-efficiency wireless energy transmission using magnetic resonance based on negative refractive index metamaterial," *Progress In Electromagnetics Research*, Vol. 106, 33–47, 2010.
17. Oktel, M. Ö. and Ö. E. Müstecaphoğlu, "Electromagnetically induced left-handedness in a dense gas of three-level atoms," *Phys. Rev. A*, Vol. 70, 053806, 2004.
18. Thommen, Q. and P. Mandel, "Electromagnetically induced left handedness in optically excited four-level atomic media," *Phys. Rev. Lett.*, Vol. 96, 053601, 2006.
19. Thommen, Q. and P. Mandel, "Left-handed properties of erbium-doped crystals," *Opt. Lett.*, Vol. 31, 1803–1805, 2006.
20. Shen, J. Q., Z. C. Ruan, and S. He, "How to realize a negative refractive index material at the atomic level in an optical frequency range?," *J. Zhejiang Univ. Science*, Vol. 5, 1322–1326, China, 2004.
21. Shen, J. Q., "Negatively refracting atomic vapor," *J. Mod. Opt.*, Vol. 53, 2195–2205, 2006.
22. Shen, J. Q., "Three-dimensionally isotropic negative refractive index assisted by two-photon resonance via quantum coherence," *Appl. Phys. Lett.*, Vol. 101, 181102, 2012.
23. Shen, J.-Q., "Gain-assisted negative refractive index in a quantum coherent medium," *Progress In Electromagnetics Research*, Vol. 133, 37–51, 2013.
24. Dutta, B. K. and P. K. Mahapatra, "Role of incoherent pumping scheme on gain without population inversion in four-level systems," *Phys. Scr.*, Vol. 77, 025403, 2008.
25. Mahmoudi, M., S. W. Rabiei, L. Safari, and M. Sahrai, "Gain-assisted superluminal propagation via incoherent pump field," *Laser Phys.*, Vol. 19, 1428–1433, 2009.
26. Budriga, O., "Incoherent pump influence on the transient gain in a V-type system with spontaneously generated coherence," *Eur. Phys. J.* D, Vol. 65, 581–585, 2011.
27. Johansson, I., "Spectra of the alkali metals in the lead-sulfide region," *Ark. Fys.*, Vol. 20, 135–146, 1961.
28. Weber, K.-H. and C. J. Sansonetti, "Accurate energies of nS, nP, nD, nF, and nG levels of neutral cesium," *Phys. Rev. A*, Vol. 35, 4650–4660, 1987.
29. Burns, K., K. B. Adams, and J. Longwell, "Interference measurements in the spectra of neon and natural mercury," *J. Opt. Soc. Am.*, Vol. 40, 339–344, 1950.

30. Haroche, S., "Etude théorique et expérimentale des propriétés physiques d'atomes en interaction avec des photons de radiofréquence," ("Theoretical and experimental studies of physical properties of atomic interaction with photons at radio frequencies (I),"), *Ann. Phys.*, Vol. 6, 189–326, Paris, 1971.
31. Haroche, S., "Etude théorique et expérimentale des propriétés physiques d'atomes en interaction avec des photons de radiofréquence," ("Theoretical and experimental studies of physical properties of atomic interaction with photons at radio frequencies (II),"), *Ann. Phys.*, Vol. 6, 327–387, Paris, 1971.
32. Jackson, J. D., *Classical Electrodynamics*, 3rd Edition, Chap. 4, 159–162, John Wiley & Sons, New York, 2001.
33. Cook, D. M., *The Theory of the Electromagnetic Field*, Chap. 11, Prentice-Hall, Inc., New Jersey, 1975.
34. Zhu, Y. and J. Lin, "Sub-doppler light amplification in a coherently pumped atomic system," *Phys. Rev.* A, Vol. 53, 1767–1774, 1996.
35. Lukin, M. D., M. Fleischhauer, A. S. Zibrov, H. G. Robinson, V. L. Velichansky, L. Hollberg, and M. O. Scully, "Spectroscopy in dense coherent media: Line narrowing and interference effects," *Phys. Rev. Lett.*, Vol. 79, 2959–2962, 1997.
36. Li, Y. and M. Xiao, "Electromagnetically induced transparency in a three-level Λ-type system in rubidium atoms," *Phys. Rev.* A, Vol. 51, R2703–R2706, 1995.
37. Truscott, A. G., M. E. J. Friese, N. R. Heckenberg, and H. Rubinsztein-Dunlop, "Optically written waveguide in an atomic vapor," *Phys. Rev. Lett.*, Vol. 82, 1438–1441, 1999.
38. Zhao, H., S. Mei, and J. Shen, "Influence of vapor pressure and Doppler effect on the optical property of a coherent atomic vapor," *Appl. Phys.*, Vol. 3, 18–25, 2013 (in Chinese).
39. Nottelmann, A., C. Peters, and W. Lange, "Inversionless amplification of picosecond pulse due to Zeeman coherence," *Phys. Rev. Lett.*, Vol. 70, 1783–1786, 1993.
40. Field, J. E., K. H. Hahn, and S. E. Harris, "Observation of electromagnetically induced transparency in collisionally broadened lead vapor," *Phys. Rev. Lett.*, Vol. 67, 3062–3065, 1991.
41. Li, Y., S. Jin, and M. Xiao, "Observation of electromagnetically induced change of absorption in multilevel rubidium atoms," *Phys. Rev.* A, Vol. 51, R1754–R1757, 1995.
42. Éntin, V. M., I. I. Ryabtsev, A. E. Boguslavskiĭ, and I. M. Beterov, "Experimental implementation of a four-level N-type scheme for

the observation of electromagnetically induced transparency," *JETP Lett.*, Vol. 71, 175–177, 2000.

43. Li, Y. and M. Xiao, "Observation of quantum interference between dressed states in an electromagnetically induced transparency," *Phys. Rev.* A, Vol. 51, 4959–4962, 1995.
44. Wei, C. and N. B. Manson, "Observation of the dynamic stark effect on electromagnetically induced transparency," *Phys. Rev.* A, Vol. 60, 2540–2546, 1999.
45. Veselago, V. G., "The electrodynamics of substances with simultaneously negative values of ϵ and μ," *Sov. Phys. Usp.*, Vol. 10, 509–514, 1968.
46. Shen, J. Q., *Classical & Quantum Optical Properties of Artificial Electromagnetic Media*, Chap. 1, Transworld Research Network, Kerala, India, 2008.
47. Shelby, R. A., D. R. Smith, and S. Schultz, "Experimental verification of a negative index of refraction," *Science*, Vol. 292, 77–79, 2001.
48. Houck, A. A., J. B. Brock, and I. L. Chuang, "Experimental observations of a left-handed material that obeys Snell's law," *Phys. Rev. Lett.*, Vol. 90, 137401, 2003.
49. Parazzoli, C. G., R. B. Greegor, K. Li, B. E. C. Koltenbah, and M. Tanielian, "Experimental verification and simulation of negative index of refraction using Snell's law," *Phys. Rev. Lett.*, Vol. 90, 107401, 2003.
50. Duan, Z., Y. Wang, X. Mao, W.-X. Wang, and M. Chen, "Experimental demonstration of double-negative metamaterials partially filled in a circular waveguide," *Progress In Electromagnetics Research*, Vol. 121, 215–224, 2011.
51. Thomas, J. R. and A. Ishimaru, "Wave packet incident on negative-index media," *IEEE Trans. Antennas Propag.*, Vol. 53, 1591–1599, 2005.
52. Berman, P. R., "Goos-Hänchen shift in negatively refractive media," *Phys. Rev.* E, Vol. 66, 067603, 2002.
53. Qing, D.-K. and G. Chen, "Goos-Hänchen shifts at the interfaces between left- and right-handed media," *Opt. Lett.*, Vol. 29, 872–874, 2004.
54. Martin, W. C. and R. Zalubas, "Energy levels of sodium, Na I through Na XI," *J. Phys. Chem. Ref. Data*, Vol. 10, 153–195, 1981.